Journal of New Technology and Materials (JNTM)
J. New Technol. Mater.
Vol. 10, N°01 (2020)10-17

OEB Univ. Publish. Co.

Effect of silver material on the performance of microstrip antenna arrays

K. Prahlada Rao[a*], Vani R. M[b] and P. V. Hunagund[a]

[a]*Department of PG Studeis and Research in Applied Electronics, Gulbarga Univesity, Gulbarga 585106, India*

[b]*University Science Instrumentation Center, Gulbarga Univesity, Gulbarga 585106, India*

*Corresponding author, email: pra_kaluri@rediffmail.com

Received date: Oct. 10, 2019 ; revised date: Jan. 04, 2020 ; accepted date: Feb. 02, 2020

Abstract

In this paper the effect of silver coating on the performance of microstrip antenna array is examined. The objective of the research study in this paper is to depict the enhanced performance of microstrip antenna array in the presence of silver material coating. The two element conventional microstrip antenna array designed at 6 GHz is resonating at simulated and measured frequencies of 5.9 and 5.53 GHz with a good return losses. It is producing simulated and measured narrow bandwidth of 2.11 and 2.35 % and high values of simulated and measured mutual coupling of -16.99 and -17.83 dB. The proposed microstrip antenna array is producing enhanced simulated and measured bandwidth of 17.28 and 17.72 % and reduced simulated and measured mutual coupling of –26.61 and 24.95 dB. In addition, good amount of reduction in backward power and increase of forward power indicate improved performance of proposed microstrip antenna array. The microstrip antenna arrays are designed and simulated using Mentor Graphics IE3D software. The thickness of silver deposition is equal to 30 nm. The dielectric substrate used to design and fabricate microstrip antenna arrays is FR-4 glass epoxy. The measured results of the fabricated antenna arrays are obtained using vector network analyzer. The components of the antenna are radiating patch, quarter wave transformer, transmission lines of 50, 70 and 100 Ω, coupler, feed line, dielectric substrate and ground plane.

Keywords: Microstrip antenna array; Mutual coupling; Radiation pattern; Silver coating.

1. Introduction

Nanoscience and nanotechnology are one of the fastest emerging technologies in the recent past. They deal with the study, making and application of extremely small things less than 100 nm in dimension. It deals with the design, characterization and production of structures, devices and systems by controlled manipulation of size and shape at the nanometre scale that produces structures, devices and systems with novel or superior characteristics or properties. [1-2]

The advent of microstrip antennas has revolutionized the field of microwave antennas to a great extent because of their small size, low cost, ease of fabrication and good compatibility with other electrical devices. Microstrip antennas are made of radiating patch, dielectric substrate and ground plane. The dielectric substrate is placed in between the radiating patch and ground plane with radiating patch on top of dielectric substrate. However these antennas also suffer from few disadvantages like narrow bandwidth and excitation of surface waves in the dielectric substrate. The surface wave excitation leads to high levels of interference between the antenna elements, which are very much necessary to be brought down. [3-7].

In [8], Fabio Urbani *et al* have reported the performance of microstrip antenna with an iron film patch of ultra thickness 10 nm. The antenna is fabricated on a double side polished silicon substrate. The antenna is seen to show a response peak greater than 10 dB at 14.5 GHz. The ultra wide bandwidth produced is equal to 1 GHz. Iron wire with 127 μm diameter and 99.999 % purity is used as the catalyst source. In [9], Maria Roo Ons *et al* have designed a transparent microstrip patch mounted on the surface of a solar module in the 3.5 GHz band. The patch has a thin sheet of clear polyester with an amorphous silicon coating. The measured bandwidth is found to be 154 MHz for the transparent patch and 302 MHz for the copper patch. The corresponding 10 dB bandwidths are equal to 4.3 and 8.3 % respectively. The gain values for the transparent and copper patches are equal to 3.96 and 5.8 dB respectively. The corresponding radiation efficiencies are 50 and 76 % respectively. In [10], Fabio Urbani *et al* have reported on experimental characterization of microstrip antennas with the radiating patch composed entirely of nano films. The four radiating patches are chromium and aluminium each of 15 nm thick, nickel and titanium each of 20 nm thick. The nano films are excited through aperture coupled feeding method. As per the return loss plot, only aluminium thin film patch structure can be classified as antenna. The other structures are classified as resonators. The aluminium thin film structure is producing bandwidth of 660 MHz. The performance of aluminium thin film structure is further investigated using over the air performance to measure the magnitude and direction of radiated energy. The antenna showed a gain of 5 dBi and good radiation properties. In [11], Jai Verdhan Chauhan *et al* have proposed a nano dot antenna array operating in the frequency range 30 – 70 GHz. Epoxy resin is used as substrate. Two microstrips

are present in the centre of the substrate, one lengthwise and the other width wise. The other epoxy substrate is used to make the sandwich. An array of nine nanodots of gold material of radius 100 nm is deposited on the surface of second substrate. The antenna is found to resonate at three frequencies – 38, 48 and 67 GHz respectively. An impedance bandwidth of 2 – 3 GHz is produced. The proposed antenna can be used for wide band applications. In [12], Rajendra Patil *et al* have reported experimental characterization of microstrip patch antenna with silver nanofilm of thickness 30 nm. The silver radiating nano film is fed by proximity coupled feeding technique. The silver nano film is deposited on top of circular radiating patch. An enhanced bandwidth of 2.71 GHz (22.39 %) with return loss of -20.41 dB is obtained at the resonant frequency of 12.1 GHz. The factors contributing to the increase in bandwidth are increase in surface resistance and skin depth. In [13], Arshad Hassan *et al* have reported the design of of a high gain antenna operating over dual band of 900 MHz and 2.4 GHz using conductive ink of silver nanoparticles to print the proposed antenna on 50 micron thick, transparent and flexible polyethyleneterephthalate (PET) substrate. The antenna structure comprises of Z-shaped radiating monopole antenna fed by co-planar waveguide feeding technique. The PET substrate has dielectric constant of 2.8 and loss tangent of 0.003. High gains of 16.74 and 16.24 dBi are obtained at 900 MHz and 2.4 GHz respectively. The fractional bandwidths obtained at the corresponding frequencies are 23.33 and 11.66 % respectively. The proposed antenna is well suited for wearable devices requiring dual Wi-Fi band. In [14], S. A. Mohasseib *et al* have studied the performance of a low profile wide band waveguide fed monopole antenna at 20 GHz and printed using silver nanoparticle ink on polyethyleneterephthalate and Epson paper substrates. A conductivity of 1.8×10^7 S/m is obtained leading to superior antenna performance with gain and antenna radiation efficiency of 1.67 dB and 96 %. Using antenna on Epson paper substrate is showing bandwidth extending from 17.18 – 24.3 GHz leading to a fractional bandwidth of 34.34 %. In [15], Mahesh C. P *et al* have designed microstrip antenna for wireless applications by loading zinc nanoparticles on rectangular patch of proposed antenna. The nano antenna is resonating at five frequencies and their corresponding bandwidths are 3.4 – 3.9 GHz (13.88 %), 4.2 – 5.2 GHz (22.22 %), 5.5 – 7.1 GHz (26.44 %), 7.6 – 8.8 GHz (16 %) and 8.95 – 9.4 GHz (4.97 %) respectively. Gain of the antenna is enhanced to 5 dB. In [16], Mahesh C. P *et al* have designed microstrip antenna
of equilateral triangular radiating patch with iron nanoparticles loaded on the patch. The nano antenna is resonating at four frequencies and their corresponding bandwidths are 3.9 – 4.05 GHz (3.65 %), 5.9 – 6.3 GHz (6.55 %), 6.9 – 8.8 GHz (26.02 %) and 9.5 – 12 GHz (22.12 %) respectively. Gain of the antenna is enhanced to 5.12 dB. In [17], Seung Yoon Lee *et al* have performed a review on transparent nano patterned antennas classified by various materials in terms of optical transmittance and sheet resistance. Graphene nano carbon based patch antennas designed in microwave frequency are producing radiation efficiency of 8 %. On the other hand, using plasmonic propagation in the THz frequency are yielding antenna efficiency of 60 %. Onion like carbon and multi wall carbon nano tube film based dipole antennas are exhibiting peak gains of -1.48 and -2.76 dBi. The copper film based antenna is featuring a peak gain of 3.5 dBi at 2.4 GHz. Transparent conductive oxides (TCO) based antennas with four films (ITO, FTO, AgHT-4, AgHT-8) with sheet resistances of 10, 24, 4.5 and 8 Ω/sq are showing wide bandwidth property. FTO is providing the highest bandwidth while ITO is giving the best performance of return loss.

The newness in the present research study is the deposition of silver metal on the entire copper area of microstrip antenna array in the ground plane and on the surface. In the previous published papers, silver was deposited on certain parts of the copper area like radiating patch, feed line etc. Additionally, a better mitigated value of mutual coupling of -26.61 dB is produced in the present research study compared to the previous published papers.

2. Materials and methods

In the first step, conventional microstrip antenna array is designed. The design frequency of conventional microstrip antenna array is 6 GHz. FR-4 glass epoxy is employed as dielectric substrate which has dielectric constant of 4.2 and loss tangent of 0.0245. The height of the dielectric substrate is 1.6 mm. Conventional microstrip antenna array has two identical rectangular radiating patches fed by corporate feeding technique. The radiating patches of conventional microstrip antenna array are separated by quarter wavelength, where the wavelength is calculated at the design frequency of 6 GHz. The dimensions of the patch are 15.73 mm × 11.76 mm. The schematic of conventional microstrip antenna array is depicted in Figure 1. The schematic in Figure 1 is used to determine the return loss characteristics of

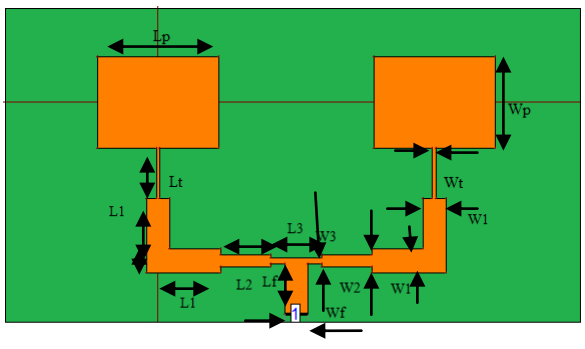

Figure 1. Schematic of conventional microstrip antenna array.

The width (Wp) of each of the radiating patches is calculated by using equation (1)

$$\frac{c}{2f_r\sqrt{\frac{\varepsilon_r+1}{2}}} \quad (1)$$

In equation (1), c is velocity of light equal to 3×10^8 m/sec, f_r is the design frequency equal to 6 GHz and ε_r is the dielectric constant or relative permittivity of the dielectric substrate equal to 4.2. Substituting the values of appropriate parameters in equation (1), the width of the radiating patch (Wp) is equal to 11.76 mm.

The length of the radiating patch (Lp) is calculated by using the equation (2)

$$L_p = L_{eff} - 2\,\Delta l \quad (2)$$

L_{eff} is calculated by using equation (3)

$$L_{eff} = \frac{c}{2f_r\sqrt{\varepsilon_e}} \quad (3)$$

ε_e is calculated by using equation (4)

$$\varepsilon_e = \frac{\varepsilon_r+1}{2} + \frac{\varepsilon_r-1}{2}\left(\sqrt{1+\frac{12h}{W}}\right)^{-\frac{1}{2}} \quad (4)$$

In equation (4), ε_r is the dielectric constant of the substrate equal to 4.2, h is the height of the substrate equal to 1.6 mm and W is the width of the radiating patch equal to 11.76 mm.

Δl is determined by using equation (5)

$$\frac{0.412h\,(\varepsilon_e+0.3)\left(\frac{W}{h}+0.264\right)}{(\varepsilon_e-0.258)\left(\frac{W}{h}+0.8\right)} \quad (5)$$

Using equations (2), (3), (4) and (5) the length of the radiating patch (Lp) is calculated as equal to 15.73 mm. Therefore, the length and width of each of the rectangular radiating patch are equal to 15.73 and 11.76 mm respectively.

The width of the feed line (Wf) is calculated by using equations (6) and (7).

$$\frac{W}{d} = \frac{8e^A}{e^{2A}-2} \quad \text{for} \quad \frac{W}{d} < 2 \quad (6)$$

$$\frac{W}{d} = \frac{2}{\pi}\left[B-1-\ln(2B-1)+\frac{\varepsilon r-1}{2\varepsilon r}\left\{\ln(B-1)+0.39-\frac{0.61}{\varepsilon r}\right\}\right]$$

$$\text{for } \frac{W}{d} > 2 \quad (7)$$

In equations (6) and (7)

$$A = \frac{Zo}{60}\sqrt{\frac{\varepsilon r+1}{2}} + \frac{\varepsilon r-1}{\varepsilon r+1}\left(0.23+\frac{0.11}{\varepsilon r}\right) \quad (8)$$

$$B = \frac{377\pi}{2Zo\sqrt{\varepsilon r}} \quad (9)$$

In equation (8), Zo is the characteristic impedance equal to 50 Ω and εr is the dielectric constant of the substrate equal to 4.2. In the present research at the design frequency of 6 GHz, $\frac{W}{d}$ is equal to 1.979 < 2. d being the height of the substrate equal to 1.6 mm, hence width of the feed (W) is equal to 6.52 mm.

The length of the feed is calculated by using equations (10), (11), (12), (13) and (14) respectively.

$$\lambda g = \frac{\lambda o}{\sqrt{\varepsilon eff}} \quad (10)$$

In equation (10), λg is the guide wavelength, λo is the free space wavelength and εeff is calculated by using equation (11).

$$\varepsilon eff = \varepsilon r - \frac{\varepsilon r-\varepsilon e}{1+g\left(\frac{f}{fp}\right)^2} \quad (11)$$

In equation (11), εr is the dielectric constant of the substrate equal to 4.2, εe is calculated by using equation (4), g is calculated by using equation (12), f is the design frequency equal to 6 GHz and fp is calculated by using equation (13).

$$g = \left(\frac{Zo-5}{60}\right)^{\frac{1}{2}} + 0.004Zo \quad (12)$$

In equation (12), Zo is the characteristic impedance equal to 50 Ω.

$$fp = \frac{Zo}{2\mu oh} \quad (13)$$

In equation (13), Zo is the characteristic impedance equal to 50 Ω, μo is permeability of free space equal to $4\pi\times10^{-7}$ H/m and h is the height of the dielectric substrate equal to 1.6 mm. The length of the feed is commonly taken as $\lambda g/4$ in order to keep minimum loss in feed line. However, the length of the feed line can be extended to any value as it acts as a connecting link between patch and source. Hence the length of the feed line is calculated as equal to 6.52 mm.

The feed designed as per the above procedure is of 50 Ω. This can be connected at the midpoint along the width of the rectangular patch. However, the impedance offered by the patch at the midpoint may not be equal to 50 Ω. Hence the feed line need not have to be connected at the midpoint as impedance mismatch occurs. In such cases a quarter wave transformer must be used between the patch and the feed line. Equation (14) is employed to determine the impedance (Rin) at the midpoint along the width of the patch.

$$Rin = \left[\frac{(120\lambda)^2+\left(\frac{377h}{\sqrt{\varepsilon rL}}\right)^2\tan^2\beta l}{240\times L\times\lambda o(1+\tan^2\beta l)}\right] \quad (14)$$

In equation (14), λ is the wavelength at the design frequency of 6 GHz, h is the height of the substrate equal to 1.6 mm, εr is the dielectric constant of the substrate equal to 4.2, L is length of the patch, λo is the free space wavelength. β and l are given by equations (15) and (16).

$$\beta = \frac{2\pi\sqrt{\varepsilon r}}{\lambda o} \quad (15)$$

In equation (15), εr is the dielectric constant of the substrate equal to 4.2 and λo is the free space wavelength.

$$l = \frac{\theta\pi}{180\beta} \quad (16)$$

The impedance of the quarter wave transformer (Zt) is calculated by using equation (17).

$$Zt = \sqrt{Rin \times Zo} \quad (17)$$

The length of the quarter wave transformer is determined by using equations (10) to (13). The width of the quarter wave transformer is determined by using equations (6) to (9). Therefore, the dimensions of the quarter wave transformer for the present research work are calculated as equal to 6.47 and 0.47 mm respectively.

The dimensions of 70 and 100 Ω transmission lines are determined on the same lines as for quarter wave transformer, except the values of Zo are equal to 70 and 100 Ω. Hence the dimensions of 70 and 100 Ω transmission lines are equal to 6.54 mm × 1.62 mm and 6.56 mm × 0.7 mm respectively.

All the dimensions of conventional microstrip antenna array are depicted in Table 1.

Table 1: Dimensions and values of conventional microstrip antenna array

Dimension	Value (mm)
Length of the patch (Lp)	15.73
Width of the patch (Wp)	11.76
Length of the quarter wave transformer (Lt)	6.47
Width of the quarter wave transformer (Wt)	0.47
Length of the 50Ω line (L1)	6.52
Width of the 50Ω line (W1)	3.05
Length of the coupler	3.05
Width of the coupler	3.05
Length of the 70Ω line (L2)	6.54
Width of the 70Ω line (W2)	1.62
Length of the 100Ω line (L3)	6.56
Width of the 100Ω line (W3)	0.70
Length of the feed line (Lf)	6.52
Width of the feed line (Wf)	3.05

By maintaining the same distance between the two adjacent antenna elements as λ/4, the parameter mutual coupling can be measured by exciting the two antenna elements separately as shown in Figure 2. The two antenna elements are assumed to be fed with the same amount of power.

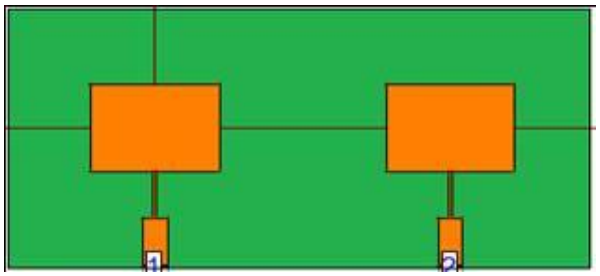

Figure 2. Setup of conventional microstrip antenna array for mutual coupling measurement

The proposed microstrip antenna array is designed by modifying conventional microstrip antenna array in such a way that a thin layer of silver material is placed on top of the entire copper area of conventional microstrip antenna array. The schematic of proposed microstrip antenna array is depicted in Figure 3. The thickness of silver deposited is equal to 30 nm. The grey part of the schematic in Figure 3 indicates the silver coating on top of entire copper area. The schematic in Figure 3 is used to evaluate the return loss characteristics of proposed microstrip antenna array.

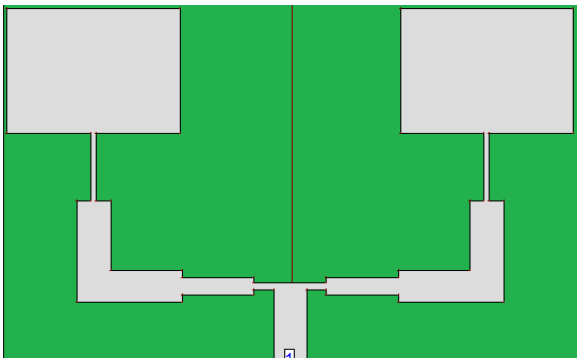

Figure 3. Schematic of proposed microstrip antenna array.

To measure the mutual coupling values of proposed microstrip antenna array, silver material of thickness 30 nm is deposited on the entire copper area of schematic of Figure 2. Figure 4 shows the schematic employed to determine the variation in mutual coupling values after the deposition of silver coating. In Figure 4 the grey part shows the silver placed on top of entire copper area.

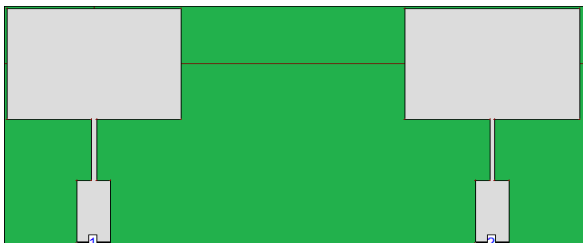

Figure 4. Setup of proposed microstrip antenna array for mutual coupling measurement

The skin depth of silver material is calculated by using equation (18)

$$\frac{1}{\sqrt{\pi f \mu \sigma}} \quad (18)$$

The skin depth of silver material calculated at the resonant frequency of 5.53 GHz is equal to 728 μm. Hence thickness of silver deposition lesser than the skin depth is selected equal to 30 nm.

Figures 5, 6, 7 and 8 depict the photographs of the fabricated microstrip antenna arrays.

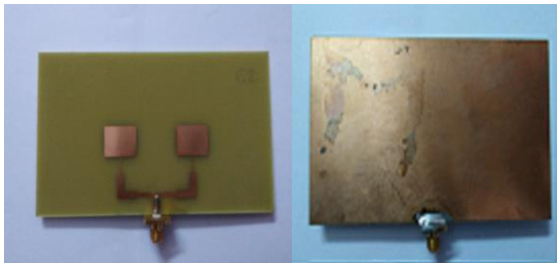

Figure 5. Photograph of conventional microstrip antenna array.
(a) Front view (b) Back view

Figure 6. Photograph of setup of conventional microstrip antenna array for mutual coupling measurement
(a) Front view (b) Back view

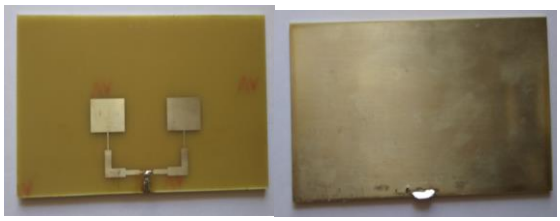

Figure 7. Photograph of proposed microstrip antenna array.
(a) Front view (b) Back view

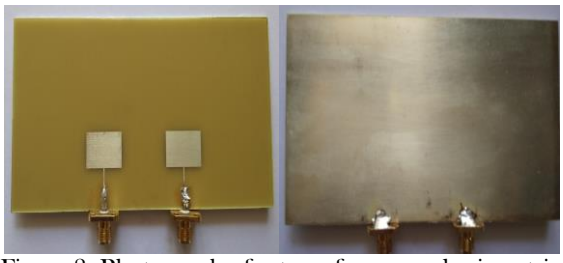

Figure 8. Photograph of setup of proposed microstrip antenna array for mutual coupling measurement.
(a) Front view (b) Back view

3. Results and discussion

The performances of conventional and proposed microstrip antenna arrays are differentiated in terms of parameters – resonant frequency, return loss, mutual coupling, forward and backward powers. Figure 9 depicts the graph of simulated and measured return loss characteristics versus frequency of conventional microstrip antenna array. The return loss is designated by S11.

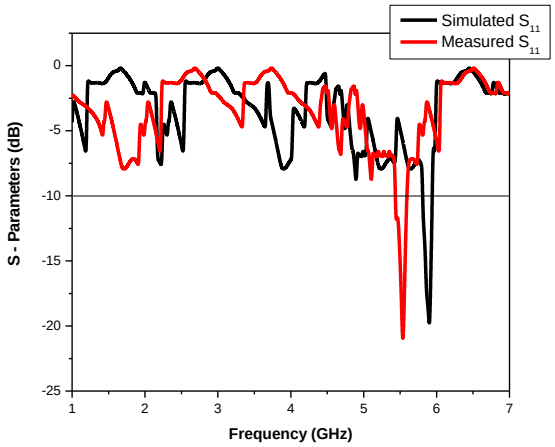

Figure 9. Plot of simulated and measured return loss versus frequency of conventional microstrip antenna array.

Figure 9 shows that the simulated and measured values of resonant frequency of conventional microstrip antenna array are 5.9 and 5.53 GHz respectively. The corresponding simulated and measured return losses are equal to -20.44 and -21.23 dB respectively. From the return loss graph the parameter bandwidth is calculated. The lower frequency is subtracted from upper frequency where the return loss is equal to – 10 dB to calculate the bandwidth. The lower and upper frequencies are located on either side of the resonant frequency. The conventional microstrip antenna array is producing simulated and measured values of bandwidth equal to 125 and 130 MHz respectively. The bandwidth (%) is determined by using equation (19)

$$\frac{Bandwidth}{Resonant\ frequency} \times 100\% \quad (19)$$

Hence conventional microstrip antenna array is producing simulated and measured bandwidth of 2.11 and 2.35 % respectively. As the bandwidth of conventional microstrip antenna array is very narrow it is very much required to enhance it.

Figure 10 depicts the simulated and measured mutual coupling versus frequency characteristics of conventional microstrip antenna array.

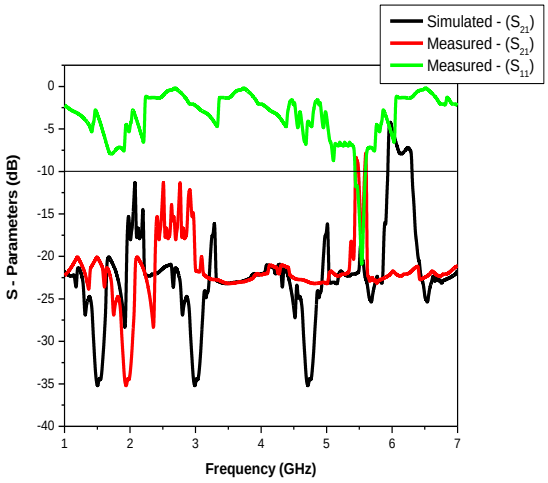

Figure 10. Plot of simulated and measured mutual coupling versus frequency of conventional microstrip antenna array.

From Figure 10 we see that the simulated and measured values of mutual coupling (S21) of conventional microstrip antenna array at the simulated and measured resonant frequencies of 5.9 and 5.53 GHz are equal to -16.99 and -17.83 dB respectively. The values of mutual coupling are very high and detrimental and need to be decreased. Additionally, we can see that the graphs of measured return loss and mutual coupling versus frequency of conventional microstrip antenna array are crossing each other at the measured resonant frequency of 5.53 GHz. This means that there is interference between the transmitting element 1 and the receiving element 2 of conventional microstrip antenna array. Hence there is no proper transmission and reception of information between the transmitting element 1 and the receiving element 2 of conventional microstrip antenna array.

Figure 11 depicts the graphs of simulated return loss and mutual coupling versus frequency of proposed microstrip antenna array.

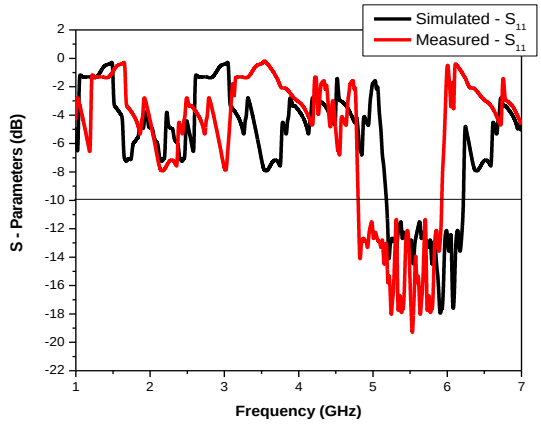

Figure 11. Plot of simulated and measured return loss versus frequency of proposed microstrip antenna array.

The graph in Figure 11 depicts that the proposed microstrip antenna array is resonating at simulated and measured fundamental frequency of 5.9 and 5.53 GHz. The simulated and measured return losses produced at the corresponding resonant frequencies of 5.9 and 5.53 GHz are equal to -18.27 and -19.98 dB. The simulated and measured bandwidths obtained at 5.9 and 5.53 GHz are equal to 1.02 and 1.1 GHz respectively. Therefore, the simulated and measured bandwidth (%) of proposed microstrip antenna array are equal to 17.28 and 17.72 % respectively. Hence the bandwidth (%) of proposed microstrip antenna array is greater than that produced by conventional microstrip antenna array. Therefore, proposed microstrip antenna array is a better antenna than conventional microstrip antenna array in terms of bandwidth.

Figure 12 depicts the simulated and measured mutual coupling versus frequency characteristics of proposed microstrip antenna array.

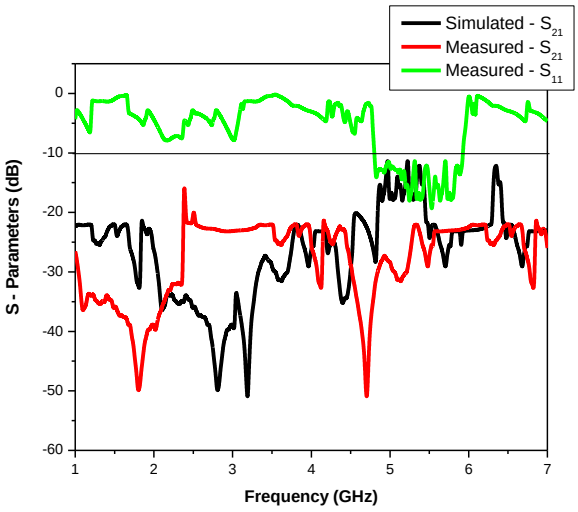

Figure 12. Plot of simulated and measured mutual coupling versus frequency of proposed microstrip antenna array.

From Figure 12 we see that the simulated and measured values of mutual coupling (S21) of proposed microstrip antenna array at the resonant frequencies of 5.9 and 5.53 GHz are -26.61 and -24.95 dB. Thus the value of mutual coupling is decreased with the introduction of silver coating. Additionally, we can also see that the graphs of measured return loss and mutual coupling versus frequency are not overlapping with each other at the resonant frequency of 5.53 GHz. This means that there is less interference between the transmitting element 1 and the receiving element 2 in proposed microstrip antenna array compared to that in conventional microstrip antenna array. Hence there is better transmission and reception of information between the transmitting element 1 and the receiving element 2 in proposed microstrip antenna array compared to that in conventional microstrip antenna array. Hence proposed microstrip antenna array is a better candidate than conventional microstrip antenna array in terms of mutual coupling.

The radiation patterns of conventional and proposed microstrip antenna arrays are shown in Figure 13.

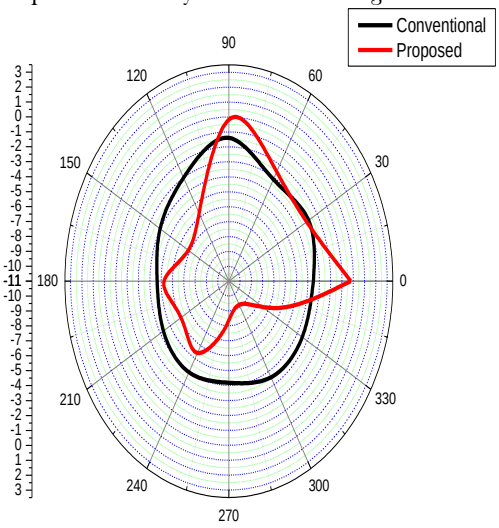

Figure 13. Plot of radiation patterns of conventional and proposed microstrip antenna arrays.

The forward power radiated is measured at the angle of 90^0 and the backward power at the angle of 270^0. In the case of conventional microstrip antenna array, the forward and backward powers measured are equal to -1.31 and -4.18 dB respectively. The corresponding powers radiated by proposed microstrip antenna array are -0.5 and -8 dB respectively. We see that proposed microstrip antenna array is radiating increased power in the forward direction and lesser power in the backward direction compared to its counterpart i.e. conventional microstrip antenna array. Hence proposed microstrip antenna array is a better radiator than conventional microstrip antenna array in terms of forward and backward powers.

Front to back ratio is calculated by using equation (20)

Front to Back ratio (dB) = Power radiated in the forward direction (dB) – power radiated in the backward direction (dB). (20)

The calculated values of front to back ratio of conventional and proposed microstrip antenna arrays are equal to 2.87 and 7.5 dB. As front to back ratio of proposed microstrip antenna array is greater than that of conventional microstrip antenna array, proposed microstrip antenna array is a better antenna in terms of front to back ratio.

Silver is so special compared to other metals because silver has the highest electrical conductivity. As to why silver is the best conductor is based on fermi sphere surface area. The conductivity in metals as per quantum free electron theory depends on Fermi sphere surface area. The Fermi sphere for any material can be plotted by taking the magnitude of Fermi velocity and radius of Fermi sphere. Mean free path is temperature dependent and Fermi velocity is temperature independent. Hence the ratio of mean free path and Fermi velocity is not constant. For silver Fermi sphere surface are is more than that of other metals.

As proposed microstrip antenna array is performing better than conventional microstrip antenna array in terms of bandwidth, mutual coupling, front power, backward radiation and front to back ratio, hence proposed microstrip antenna array is considered as a superior candidate compared to its counterpart conventional microstrip antenna array

Tables 2 and 3 depict the summarized simulated and measured results of conventional and proposed microstrip antenna arrays.

Table 2: Summarized simulated and measured results of conventional microstrip antenna array.

Parameter	Resonant Frequency (GHz)	Return Loss (dB)	Band Width (MHz)	Band Width (%)	Mutual Coupling (dB)
Simulated	5.19	-20.44	125	2.11	-16.99
Measured	5.53	-21.23	130	2.35	-17.83

Table 3: Summarized simulated and measured results of proposed microstrip antenna array.

Parameter	Resonant Frequency (GHz)	Return Loss (dB)	Band Width (MHz)	Band Width (%)	Mutual Coupling (dB)
Simulated	5.19	-18.27	1020	17.28	-26.61
Measured	5.53	-19.98	1100	17.72	-24.95

Table 4 summarizes the results of the previous authors' work and present research study.

Table 4: Summarized results of previous authors work and present research study.

	Bandwidth (MHz)	Bandwidth (%)	Mutual Coupling (dB)
Red [8]	1000	---	---
Red [9]	154	4.3, 8.3	---
Red [10]	660	---	---
Red [11]	2000-3000	---	---
Red [12]	2710	22.39	---
Red [13]	990, 2400	23.33, 11.66	---
Red [14]	---	34.34	---
Red [15]	500, 1000, 1600, 1200, 550	13.88, 22.22, 26.44, 16, 4.97	---
Red [16]	150, 400, 1900, 2500,	3.65, 6.55, 26.02, 22.12	---
Red [17]	---	---	---
Present Research Study	1100	17.72	-26.61

4. Conclusion

In this paper, the study of performance of two element antenna array without and with silver coating is performed in terms of various parameters. The antenna arrays have been successfully designed, simulated and tested practically. The simulated and experimental results are in agreement to a good extent. The deposition of silver coating is producing enhanced bandwidth and good reduction in mutual coupling value. With reduction in back lobe power, the introduction of silver coating demonstrates the enhanced performance of proposed microstrip antenna array compared to its counterpart i.e. conventional microstrip antenna array.

References

[1] L. I. Maissel, R. G. Glang (Eds.), Handbook of Thin Film Technology, McGraw-Hill Book Company, New Yaork, USA, (1970)

[2] https://www.nanowerk.com/nanotechnology/introduction/introduction_to_nanotechnology_1.php.

[3] Constantine A. Balanis, 2nd ed., Antenna Theory, Analysis and Design, John Wiley & Sons Inc, (1997)

[4] I. J. Bahl, P. Bhartia, Microstrip Antennas, Artech House, (1980)

[5] Mentor Graphics IE3D User Manual, (2010).

[6] James Scott, Lecture Notes of EEET 1071/1127 Microwave and Wireless Passive Circuit Design, (2004)

[7] A. K. Gautam, Antenna and Wave Propagation, 5th ed., (2010)

[8] Fabio Urbani, David W. Stollberg, Amit Verma, Proc. of 2010 IEEE Nanotechnology Materials and Devices Conf., Monterey, California, USA., 12-15 Oct., 2011; 160-163.

[9] Maria Roo Ons, S. V. Shynu, Max Ammann, Sarah McCormak, Brian Norton, Electronic Letters. 47 (2011) 85-86.

[10] Fabio Urbani, David W. Stollberg, Amit Verma, IEEE Transactions on Nanotechnology. 11 (2012) 406-411.

[11] Jai Verdhan Chauhan, Abhishek Khandwal, Sunil Kumar Khah, International Journal of Emerging Technology and Advanced Engineering. 4 (2014) 336-338.

[12] Rajendra R. Patil, Vani R. M, P. V. Hunagund, International Journal of Engineering Trends and Technology. 13 (2016) 299-302.

[13] Arshad Khan, Shawkat Ali, Gul Hassan, Jinho Bae, Chong Hyun Lee, Microsystem Technologies. (2016).

[14] S. A. Mohasseib, Khaled Kirah, Edgar Dorsam, Ahmed S. G. Khalil, Hadia M. El- Hennawy, IET Microwaves, Antennas & Propagation. 11 (2017) 1572-1577.

[15] C. P. Mahesh, Madhuri Chavan, Maheshwar Sharon, Madhuri Sharon, International Journal for Research in Applied Science & Engineering. 6 (2018) 249-252.

[16] C. P. Mahesh, Pooja Mali, Maheshwar Sharon, Madhuri Sharon, International Journal for Research in Applied Science & Engineering. 6 (2018) 257-260.

[17] Seung Yoon Lee, Moogoong Choo, Sohyeon Jung, Wonbin Hong, Applied Sciences. 8 (2018) 1-13.